THE JOURNAL OF PHYSICAL CHEMISTRY A

Article

pubs.acs.org/JPCA

Mechanism and Kinetics for Ammonium Dinitramide (ADN) Sublimation: A First-Principles Study

R. S. Zhu,[†] Hui-Lung Chen,[‡] and M. C. Lin[†,§,*]

[†]Department of Chemistry, Emory University, Atlanta, Georgia 30322, United States

[‡]Department of Chemistry and Institute of Applied Chemistry, Chinese Culture University, Taipei, 111, Taiwan

[§]Center for Interdisciplinary Molecular Science, Department of Applied Chemistry, National Chiao Tung University, Taiwan

Supporting Information

ABSTRACT: The mechanism for sublimation of $NH_4N(NO_2)_2$ (ADN) has been investigated quantum-mechanically with generalized gradient approximation plane-wave density functional theory calculations; the solid surface is represented by a slab model and the periodic boundary conditions are applied. The calculated lattice constants for the bulk ADN, which were found to consist of $NH_4^+[ON(O)NNO_2]^-$ units, instead of $NH_4^+[N(NO_2)_2]^-$, agree quite well with experimental values. Results show that three steps are involved in the sublimation/decomposition of ADN. The first step is the relaxation of the surface layer with 1.6 kcal/mol energy per $NH_4ON(O)NNO_2$ unit; the second step is the sublimation of the surface layer to form a molecular $[NH_3]-[HON(O)NNO_2]$ complex with a 29.4 kcal/mol sublimation energy, consistent with the experimental observation of Korobeinichev et al.[10] The last step is the dissociation of the $[H_3N]-[HON(O)NNO_2]$ complex to give NH_3 and $HON(O)NNO_2$ with the dissociation energy of 13.9 kcal/mol. Direct formation of NO_2 (g) from solid ADN costs a much higher energy, 58.3 kcal/mol. Our calculated total sublimation enthalpy for ADN(s) → NH_3(g) + $HON(O)NNO_2$) (g), 44.9 kcal/mol via three steps, is in good agreement with the value, 42.1 kcal/mol predicted for the one-step sublimation process in this work and the value 44.0 kcal/mol computed by Politzer et al.[11] using experimental thermochemical data. The sublimation rate constant for the rate-controlling step 2 can be represented as $k_{sub} = 2.18 \times 10^{12}$ exp (−30.5 kcal/mol/RT) s^{-1}, which agrees well with available experimental data within the temperature range studied. The high pressure limit decomposition rate constant for the molecular complex $H_3N\cdots HON(O)$-NNO_2 can be expressed by $k_{dec} = 3.18 \times 10^{13}$ exp (−15.09 kcal/mol/RT) s^{-1}. In addition, water molecules were found to increase the sublimation enthalpy of ADN, contrary to that found in the ammonium perchlorate system, in which water molecules were shown to reduce pronouncedly the enthalpy of sublimation.

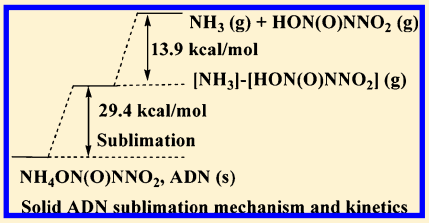

1. INTRODUCTION

Ammonium dinitramide, $NH_4N(NO_2)_2$ (ADN), a powerful oxidizer, is a potential halogen-free replacement for ammonium perchlorate as a solid rocket propellant.[1−3] ADN is known to exist in two polymorphic forms: α and β.[4] The α-ADN phase existing only in the low-pressure regime has been resolved by X-ray diffraction measurements.[5] The crystal structure of the unit cell is monoclinic with four ($[NH_4]^+[N_3O_4]^-$) molecules per unit cell. This phase is stable up to 2.0 GPa over a large range of temperatures. Because of the fact that only the α-ADN has been experimentally characterized and the β-ADN exists only at higher pressures (P > 2.0 GPa);[4] therefore, we only considered the α phase in the present study.

The activation energy for ADN sublimation is highly dependent on the experimental conditions, and it is reported to be between 26 and 43 kcal/mol.[6−10] Korobeinichev et al.[10] have carefully studied the thermal decomposition of ADN with time-of-flight (TOF) and a quadrupole mass-spectrometry (MS) at pressures of 10^{-6}, 6, 100 Torr, and 1 atm within the temperature range of 353−673 K under isothermic and nonisothermic conditions. Their results show that 90% ADN sublime in a flow reactor under the conditions of 353−413 K and 6 Torr pressure. Gaseous ADN decomposes into dinitraminic acid (HD) and ammonia at 433−673 K. Their experiment proved for the first time the existence of gaseous ADN and HD, the mechanism can be expressed as:[10]

$$\mathrm{ADN_s} \rightarrow [\mathrm{NH_3}] - [\mathrm{HN(NO_2)_2}]_g \text{ or } [\mathrm{NH_3}] - [\mathrm{HON(O)NNO_2}]_g \rightarrow \mathrm{NH_{3(g)}} + \mathrm{HN(NO_2)_{2(g)}} \text{ or } \mathrm{HON(O)NNO_2(g)}$$

The sublimation enthalpy has been estimated to be 44 kcal/mol by Politzer et al.[11] combining the computational heat of formation of $HN(NO_2)_2$ (g) and experimental heats of formation of NH_3 (g) and ADN(s). The mechanism and the energetics for the decomposition of the gaseous ADN have been computationally studied in detail by Mebel et al.,[12] whereas the kinetics for the dissociation of the $HN(NO_2)_2$ acid had been theoretically predicted by Park et al.[13] However, the kinetics and mechanism for the initial sublimation, one of the most important stages involved in the layer of burning surface

Received: August 3, 2012
Revised: September 26, 2012
Published: October 2, 2012

for ADN combustion, has not been elucidated. To understand the combustion mechanism and develop a comprehensive combustion model for this important class of energetic material, it is essential to have quantitative data for the products and energetics of the individual steps. Recently, we have studied the kinetics and mechanisms for the sublimation and decomposition of solid NH_4Cl,[14] and NH_4ClO_4(AP)[15] by first-principles and statistical-theory calculations. Our studies have illustrated convincingly that the generalized gradient approximation with the plane-wave density functional theory within the periodic boundary condition can not only reliably reproduce the experimental molecular parameters and the physicochemical characteristics of ammonium salts but also their sublimation kinetics.

In the present work, we have carried out the first quantum-chemical calculation on ADN sublimation in an attempt to elucidate the mechanism and kinetics for the process. The predicted results are compared with existing experimental data.

2. COMPUTATIONAL METHODS

The calculation has been carried out with the Vienna Ab-initio Simulation Package (VASP),[16−19] which evaluates the total energy of periodically repeating geometries on the basis of DFT with the pseudopotential approximation. For the periodic boundary condition, the valence electrons were expanded over a plane-wave basis set. The core electron calculations are performed with the cost-effective pseudopotentials implemented in VASP. The expansion includes all plane waves with their kinetic energies smaller than the chosen cutoff energy, that is $\hbar^2 n^2k^2/2m < E_{cut}$, where k is the wave vector, m is the electronic mass, and E_{cut} is the chosen cutoff energy. In this study, a cutoff energy of 500 eV was used.

Generalized gradient approximation (GGA)[20,21] with PW91 exchange-correlation functional was used for the present calculation. The Brillouin-zone (BZ) integration is sampled with 0.05 × 2 (1/Å) spacing in reciprocal space by the Monkhorst-Pack scheme,[22] with k-points grid of 4 × 2 × 4 and the Fermi-smearing σ = 0.1 eV. The equilibrium structure of the crystals is obtained by full relaxation of the ionic positions inside the unit cell with the monoclinic space group, $P2_1/c$. To minimize the interaction between the distinct slab surface in this infinitely periodic model system, a vacuum region of 40 Å was used to separate the top and bottom surfaces of the slabs.

3. RESULTS AND DISCUSSION

3.1. Lattice Constant and Geometric Parameters. To select a computationally practical and reasonable model, supercells including 4 and 8 units of $NH_4N_3O_4$ were employed for the bulk calculations and all atomic positions of the molecules were relaxed. In the ADN solid, the $HN(NO_2)_2$ acid exists as $HON(O)NNO_2$ through H··O hydrogen bonding. The calculated lattice constants are a = 7.104, 6.960 Å; b = 9.783, 11.529, Å; c = 7.335, 5.428 Å for the above models, respectively. Our results show that the calculated lattice constants, bond lengths and bond angles with 8 molecules/ion pairs (Figure 1) are in good agreement with the experimental values[5] (Table 1). Therefore, we use this model to represent the ADN crystal and the subsequent calculations are based on this model, and in the following section we mainly consider the formation mechanism of NH_3 + $HON(O)NNO_2$ instead of NH_3 + $HN(NO_2)_2$.

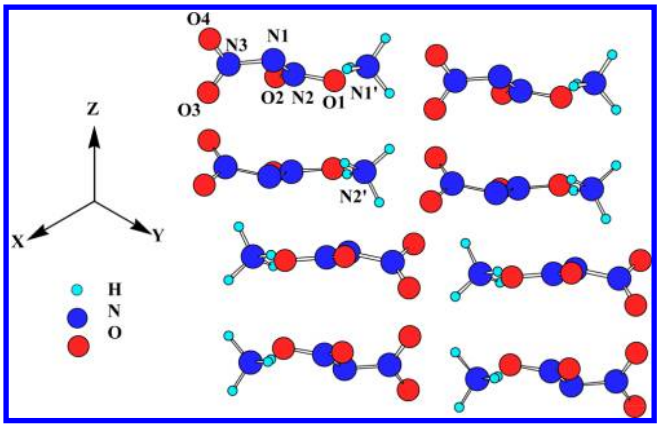

Figure 1. Optimized configuration for the relaxed 010 surface model with 8 $NH_4N(NO_2)_2$ molecules/ion pairs.

Table 1. Comparison of the Experimental and Calculated Structural Parameters for ADN in Crystal Environment, Calculated by VASP with 8 $NH_4N(NO_2)_2$ Unit Cells; Distances in Ångstroms and Angles in Degrees

parameters	calculated	expt[5]
lattice	a = 6.960	a = 6.914
constants	b = 11.529	b = 11.787
	c = 5.428	c = 5.614
R(N1−N2)	1.367	1.376
R(N1−N3)	1.359	1.359
R(N2−O1)	1.259	1.236
R(N2−O2)	1.246	1.227
R(N3−O3)	1.275	1.252
R(N3−O4)	1.242	1.223
N2−N1−N3	114.9	113.2
O1−N2−O2	123.3	123.3
O1−N2−N1	113.2	113.0
O2−N2−N1	123.3	123.3
O3−N3−O4	122.0	122.1
O4−N3−N1	125.2	125.1

3.2. Sublimation Enthalpy Change. The sublimation energy of the ADN crystal was calculated as the energy difference between a single fully optimized $NH_4ON(O)NNO_2$ molecule in the crystal and that of the gas-phase products, NH_3 + $HON(O)NNO_2$; that is,

$$\Delta H_{sub} = E[NH_3(g) + HON(O)NNO_2(g)] - [E(\text{supercell})]/X$$

where X is the number of $NH_4N_3O_4$ units in the supercell. The value obtained by one-step calculation is 42.1 kcal/mol using the 8 unit of $NH_4N_3O_4$ model. On the basis of the three step processes shown in Figure 2, the enthalpy change is predicted to be 44.9 kcal/ml, which is in excellent agreement with the value mentioned above as well as the thermochemical value of 44.0 kcal/mol predicted by Politzer et al.[11] from the computational and experimental data.

3.3. Sublimation/Decomposition Energies of NO_2 and H_3N···$HON(O)NNO_2$ from the Relaxed Top Layer. In the mass-spectrometric measurement by Korobeinichev et al.[10] for the ADN sublimation and decomposition at low pressures, the most intensive peaks are M/Z 46, 17 (NH_3), 18 (H_2O), 30 (NO) and a weak mass peak at M/Z 44 (N_2O). The ratio of the mass peaks 30 and 46 (I_{30}/I_{46}) is about 0.5, which is much

dx.doi.org/10.1021/jp307714d | J. Phys. Chem. A 2012, 116, 10836−10841

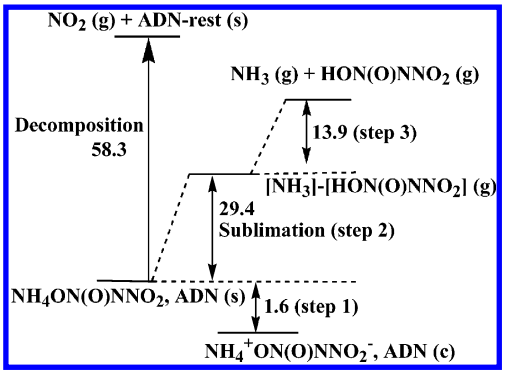

Figure 2. Schematic energy diagram (in unit kcal/mol) for the sublimation/dissociation processes of $NH_4N(NO_2)_2$. Where $NH_4N(NO_2)_2$ (c) refers to $NH_4N(NO_2)_2$ in the crystal environment; $NH_4N(NO_2)_2$ (s) represents $NH_4N(NO_2)_2$ on the relaxation surface and NH_3 (g), NO_2 (g) and $H_3N\cdots[HON(O)NNO_2]$ (g) represent those products in the gas-phase.

smaller than 6.2 in NO_2 mass-spectrum; therefore, the authors suggested that the peak with mass 46 should not be assigned to NO_2 but to ADN(g) with the peak ratios of I_{17}:I_{30}:I_{44}:I_{46} = 0.35:0.5:0.1:1. We consider both NO_2(g) and ADN(g) as potential sublimation and decomposition products because, in principle, they can compete in the first stage of sublimation/decomposition processes. The sublimation and decomposition energies E_{sub} and E_{dec} for the $H_3N\cdot\cdot HON(O)NNO_2$ complex and NO_2 molecule desorbing from the relaxed 010 surface respectively are defined as:

$$E_{sub} = [E(\text{hole}) + E_{cpx}(g)] - E_{slab}$$

$$E_{dec} = [E(\text{hole}) + E_{NO_2}(g)] - E_{slab}$$

The relaxed 010 surface here means the 010 surface created by cleaving the surface layer from the bulk material and the subsequent surface optimization to relax its atoms to reach their minimum energy positions with 40 Å vacuum space. E(hole) is the energy of the slab after eliminating an individual molecule $[H_3N\cdot\cdot HON(O)NNO_2]$ or (NO_2); $E_{NO_2}(g)$ and $E_{cpx}(g)$ are the energies of the isolated NO_2 and $H_3N\cdots HON(O)NNO_2$ in the gas phase respectively calculated in a 25 × 25 × 25 Å^3 cubic box; E_{slab} is the total energy of the slab with the 40 Å vacuum space. E_{dec} for the direct NO_2 production was predicted to be 58.3 kcal/mol, whereas E_{sub} for $H_3N\cdots HON(O)NNO_2$ desorption from the relaxed surface was predicted to be 29.4 kcal/mol. These data as shown in Figure 2 clearly indicate that the decomposition of NO_2 from the relaxed first surface layer cannot compete with the sublimation of $H_3N\cdots HON(O)NNO_2$ molecular pair because the former involves breaking a strong N−N bond. Our calculated result is in agreement with the experimental observation of Korobeinichev et al.,[10] but in their work they assigned the sublimation complex as $H_3N-HN(NO_2)_2$, which has the same mass as $H_3N\cdots HON(O)NNO_2$ and cannot be differentiated from the former. A similar conclusion has been reached for the sublimation of NH_4Cl[14] and NH_4ClO_4,[15] in which the $H_3N\cdots HCl$ and $H_3N\cdots HClO_4$ molecule pairs desorb preferentially from the relaxed surfaces, instead of the acid and base molecules desorbing individually as was assumed previously.

In our calculations for the sublimation of $H_3N\cdots HON(O)NNO_2$ as a pair, one of the top layer $NH_4N_3O_4$ molecules was pulled off along the Z axis from the relaxed 010 surface (Figure 1). The distance between the N atom (N1′) of the leaving $NH_4N_3O_4$ in the first layer and another N atom (N2′) in the second layer of $NH_4N_3O_4$ is defined as R. The minimum energy path (MEP) of sublimation (open symbol) as a function of the separation (R) is plotted in Figure 3. With the exception

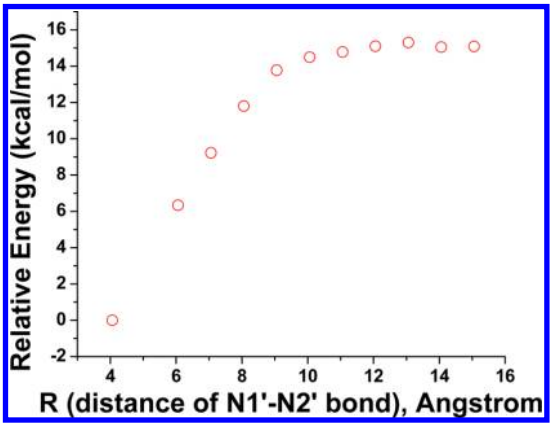

Figure 3. Relative energy for one of $NH_4N(NO_2)_2$ molecules desorbing from the relaxed crystal surface, where R represents the distance between N1′ and N2′ as the configuration indicated in the Figure 1; the open circle symbol is the calculated value.

of the N1′−N2′ distance, the other structural parameters of each point along the curve was fully optimized. No distinct intrinsic transition state was found in the calculation as in the NH_4Cl and NH_4ClO_4 cases. The result indicates that the proton gradually transfers from the NH_4^+ moiety to the $N_3O_4^-$ moiety as R is increasing during the sublimation process. At R = 11−15 Å, the sublimation energy curve reaches the asymptote with energy around 15.8 kcal/mol, which is lower than the value of 29.4 kcal/mol at R = ∞. The energy difference (13.6 kcal/mol) between the sublimation path and end point simulations arises from the slab spatial constraint. We confirmed this by recalculating the gas-phase $H_3N\cdots HON(O)NNO_2$ energy in a smaller 6.96 × 51.5 × 10.86 Å^3 box with which the sublimation energy was computed. On the basis of the energy of $H_3N\cdots HON(O)NNO_2$ in this box, the sublimation energy is 19.3 kcal/mol. If $H_3N\cdots HON(O)NNO_2$ are optimized as a gas phase in a 30 × 30 × 30 Å^3 box, the energy difference becomes 10.1 kcal/mol, which is close to the above deviation, 13.6 kcal/mol. Because of the interaction between the slabs along the X and Y directions, the geometry of $H_3N\cdots HON(O)NNO_2$ in the slab of 6.96 × 51.5 × 10.86 Å^3 with the computationally affordable 40 Å vacuum space in the Z direction does not really reach that predicted in the gas phase. This calculation can quantitatively explain why the sublimation energy of this system given in Figure 3 at the asymptotes is lower than that of at R = ∞ in Figure 2. Similar results were noted in the sublimation processes of NH_4Cl[14] and NH_4ClO_4 systems,[15] in which $H_3N\cdots HCl$ and the $H_3N\cdots HOClO_3$ pairs above their surfaces at R = 20.0 Å do not reach their real gas-phase values at R = ∞ for 3 dimensions due to the interactions between the slabs along the X and Y directions.

3.4. Proposed Sublimation/Dissociation Mechanism. On the basis of the results presented above, we suggest that the sublimation/dissociation reaction of ADN is a multistage process, taking place as shown in Scheme 1, where (c) refers to ($[NH_4]^+[N_3O_4]^-$) in the crystal environment (bulk); (s) refers to the relaxed surface, and (g) refers to the gas phase.

dx.doi.org/10.1021/jp307714d | J. Phys. Chem. A 2012, 116, 10836−10841

Scheme 1

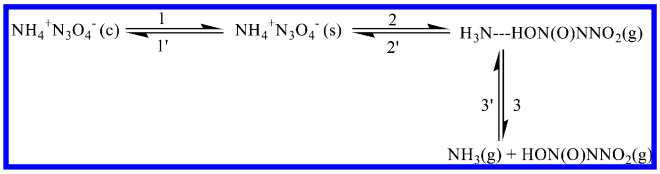

The energy diagram for this process is plotted in Figure 2. Similar to the NH_4Cl and NH_4ClO_4 systems,[14,15] the result of our calculations indicates that three steps are involved in the sublimation/decomposition process as illustrated in Scheme 1 and in Figure 2. In the first step, the $NH_4^+[ON(O)NNO_2]^-$ molecules relax from their crystal structure on the surface with only 1.6 kcal/mol relaxation energy, which is close to the value, 0.1 kcal/mol, for the NH_4ClO_4 system, but it is much lower than the value 18.7 ± 1.0 kcal/mol predicted for the NH_4Cl system; the result may be attributed to the loose lattice structures of ADN and AP. In the second step, one of the $NH_4^+[ON(O)NNO_2]^-$ ion pairs on the surface undergoes proton transfer to form a $H_3N\cdots HON(O)NNO_2$ complex and desorbs with 29.4 kcal/mol endothermicity. Our calculated results indicate that the sublimation complex $H_3N\cdots HON(O)$-NNO_2 is a more stable isomer than $H_3N\cdots HN(NO_2)_2$ by 1.3 kcal/mol at the CCSD(T)/6-311+G(3df,2p)//B3LYP/6-311+G(3df, 2p) level; $H_3N\cdots HON(O)NNO_2$ can readily convert to $H_3N\cdots HN(NO_2)_2$ with only a 5.2 kcal/mol energy barrier. The difference between the $NH_4^+[ON(O)NNO_2]^-$ and $[NH_4]^+[N(NNO_2)]^-$ structures is shown in SI-I of the Supporting Information I. In the last step, the molecular complex $H_3N\cdots HON(O)NNO_2$ (g) dissociates in the gas phase to NH_3(g) and $HON(O)NNO_2$ (g) with a relatively small energy of 13.9 kcal/mol. The energy change in the whole process, 44.9 kcal/mol, is in good agreement with the value, 42.1 kcal/mol, predicted by one-step calculation for ADN(s) → NH_3(g) + $HON(O)NNO_2$(g) as discussed in the previous section and it is also very close to 44.0 kcal/mol predicted by Politzer et al. based on a thermochemical estimation.[11]

3.5. Effect of H_2O on the Sublimation Process. In our previous study of the AP sublimation process, we investigated the effect of 1−3 H_2O molecules on the enthalpies of sublimation.[31] The results show that the sublimation energies of $(H_2O)_n\cdots NH_4/ClO_4$ (n = 0, 1, 2, 3) molecular complexes from the surface decrease with the numbers of H_2O increasing: 28.1, 21.4, 18.6, and 14.2 kcal/mol, respectively. The lowering of the sublimation enthalpies can be attributed to the formation of $NH_4^+ClO_4^-$ ionic pairs in the presence of the complexing water molecules during the desorption process as revealed by the predicted molecular structures.[31] In this work, we have studied the effect of H_2O on the sublimation of ADN also with 1−3 H_2O molecules. The calculated sublimation enthalpies are summarized and compared with those of AP in Table 2. Interestingly and contrarily to AP, the sublimation enthalpy increases in the case of ADN from 29.4 kcal/mol without water to 32.6 and 32.8 kcal/mol with 1 and 2 H_2O molecules involved; in the 3 H_2O case, the sublimation enthalpy slightly decreases to 30.0 kcal/mol. Our results can be qualitatively compared with the experimental finding that when a small amount of water was added to the ADN, the decomposition first decreased but later increased when the amount of water exceeded 5%.[32,33]

The qualitatively different H_2O effects on AP and ADN may be explained from the structures changed as shown in SI-II of the Supporting Information without H_2O and with $2H_2O$ on the surface as an example. Without H_2O, the sublimation of the top layer $NH_4^+ClO_4^-$ and $NH_4^+N_3O_4^-$ form molecular complexes, $H_3N\cdots HOClO_3$ and $H_3N\cdots HON(O)NNO_2$, respectively with similar sublimation energies, 28.1 and 29.4 kcal/mol. However, in the 2 H_2O molecules case, the sublimation product of AP is an ionic complex, $2H_2O\cdots NH_4^+/ClO_4^-$, the structural parameters of this super molecule complex ($2H_2O\cdots NH_4^+/ClO_4^-$) are similar to those in the AP crystal; however, in ADN, H_2O induces proton transfer from NH_4^+ to $N_3O_4^-$ to form the $H_3N\cdots HON(O)NNO_2\cdots 2H_2O$ complex, which costs more energy and is different from the complex formed in AP. By examination of the hydrogen bonds in $2H_2O\cdots NH_4/ClO_4^-$ and $H_3N\cdots HON(O)NNO_2\cdots 2H_2O$, one finds that the hydrogen bonds in the $2H_2O\cdots NH_4^+/ClO_4^-$ complex are stronger than those of in the $NH_4^+\cdots ON(O)$-$NNO_2^-\cdots 2H_2O$ complex resulting in the lower sublimation energies in AP.

Table 2. Comparison of H_2O Effect on the Sublimation Enthalpies for $(H_2O)_n\cdots NH_4/ClO_4$ and $(H_2O)_n\cdots NH_4/N_3O_4$ Pairs from the AP and ADN Surfaces

	Sublimation Enthalpy (kcal/mol)	
$(H_2O)_n$	ADN	AP[31]
n = 0	29.4	28.1
n = 1	32.6	21.4
n = 2	32.8	18.6
n = 3	30.0	14.2

3.6. Rate Constant Calculations. *Sublimation Process.* The sublimation process, $[(NH_4ON(O)NNO_2]_X \rightarrow [(NH_4ON(O)NNO_2]_X^* \rightarrow [(NH_4ON(O)NNO_2]_{X-1} + H_3N\cdots HON(O)NNO_2$(g), is a barrierless desorption reaction as calculated above for X = 8. The potential energy along the MEP (minimum energy path) is shown in Figure 3. We compute the rate constant based on the canonical variational transition state theory,[23]

$$k_s = \frac{k_B T}{h}\frac{Q^*}{Q}\exp(-E_0/k_B T) \quad (1)$$

Here k_B is the Boltzmann constant, T is the temperature, h is Planck's constant, E_0 is the energy of activation per molecule at 0 K, Q^*, and Q are the molecular partition function for the transition state and the reactant, respectively. The computational method for prediction of the rate constant has been discussed before[14,15] and is briefly presented below.

For the barrierless (not well-defined) transition states, the parameters were evaluated canonically for each temperature for the critical separation, $r^*(T)$, based on the maximum Gibbs free energy criterion as described in refs 24 and 25. The result shows that in the temperature range of 350−800 K within which most of the experimental temperatures lie, the transition state locates at nearly the same point at R = 13.058 Å. In the sublimation process, only the structures and frequencies of the subliming NH_4/N_3O_4 pair undergo a significant change along the reaction coordinate, other parts of the relaxed surface have minor changes. Therefore, only the frequencies of the subliming NH_4/N_3O_4 pair in the relaxed surface (reactant) and at the transition points are included in the rate constant calculation; the frequencies of vibrations of other atoms of the reactant and the transition state are effectively canceled in the partition function ratio Q^*/Q in the above-mentioned eq 1.

dx.doi.org/10.1021/jp307714d | J. Phys. Chem. A 2012, 116, 10836−10841

The key vibrational frequencies for the NH_4/N_3O_4 pair in the relaxed surface and in the transition state involved in the sublimation process are listed in SI-III of the Supporting Information.

The rate constant was calculated by the ChemRate code[26] with D_e = 29.4 kcal/mol at $R = \infty$. The predicted values presented in Figure 4 lie within the scattered experimental data.[9,10] The calculated result can be represented as: $k_{sub} = 2.18 \times 10^{12}$exp (−30.5 kcal/mol/RT) s^{-1}.

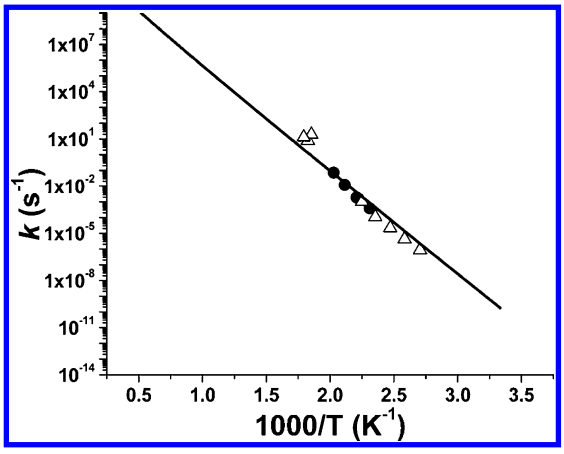

Figure 4. Predicted ADN sublimation/dissociation rate constant. Solid line is the calculated value; symbols are taken from the experimental data: ●, ref 9 and Δ, ref 10.

$H_3N\cdots HON(O)NNO_2$(g) Decomposition. After sublimation, the $H_3N\cdots HON(O)NNO_2$(g) molecular complex can readily fragment to $HON(O)NNO_2$(g) + NH_3(g) with 13.9 endothermicity predicted at the CCSD(T)/6-311+G(3df, 2p)//B3LYP/6-311+G(3df,2p) level at 0 K. We also calculate the dissociation energy of $H_3N\cdots HON(O)NNO_2$(g) using high level CBS-APNO[34] and CBS-QB3[35] methods, calculated values are 14.1 and 14.3 kcal/mol at the above two levels, respectively. These 0 K values are slightly larger than the reported experimental activation energy 11.5 kcal/mol[10] in the temperature range of 353 −413 K due to the nature of the variational transition states whose entropy of activation (or equivalently the A-factor) becomes smaller at higher temperatures resulting in a smaller value of activation energy than the predicted 0 K energy barrier.

The dissociation rate constant for this complex is calculated by using the variational RRKM theory[27−29] implemented in the Variflex code.[30] The molecular parameters employed in the calculation are listed in SI−IV of the Supporting Information; SI−V displays the variational dissociation curve computed at the B3LYP/6-311+G(3df, 2p) level and the fitted values using the Morse potential. Energies at the CCSD(T)/6-311+G(3df, 2p)//B3LYP/6-311+G(3df,2p) level are used in the rate calculation. Figure 5 compares the calculated rate constants in the range of 10^{-6} to 760 Torr Ar pressure and the available experimental values measured under 10^{-6} to ∼100 Torr pressure;[10] the agreement appears to be reasonable. The predicted result shows a strong pressure dependence as one would expect, although such an effect was not clearly revealed by the flow study of Korobeinichev and co-workers.[10] As also anticipated, this process is considerably faster than the desorption of the $H_3N\cdots HON(O)NNO_2$ complex in step 2 due to the more than 15 kcal/mol lower barrier. The high

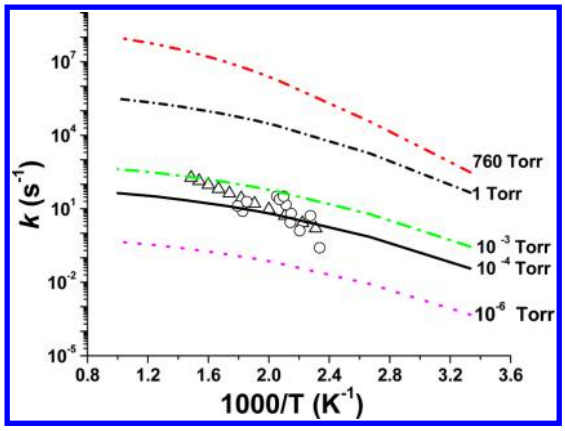

Figure 5. Decomposition rate for $H_3N\cdots HON(O)NNO_2$ (g) → NH_3 (g) + $HON(O)NNO_2$ (g). Open circle (○) values are the experimental measured data in 10^{-6} to ∼100 Torr Ar (ref 10); open triangle (Δ) data taken from the suggested equation (ref 10) $k = 10^6 \times$ exp (−11.5 kcal/mol/RT) s^{-1}. Lines from bottom to top are the calculated values in this work from 10^{-6} to 760 Torr Ar.

pressure limit rate constant for this dissociation of the molecular complex can be expressed by $k_{dec} = 3.18 \times 10^{13}$ exp (−15.09 kcal/mol/RT) s^{-1}.

4. CONCLUSIONS

In this article, we have performed first-principles calculations using the plane-wave DFT for elucidation of the sublimation/dissociation mechanism of $NH_4N(NO_2)_2$. The result of our calculations indicates that three distinct steps are involved in the sublimation process. In the first step, $NH_4^+N_3O_4^-$ molecules relax from their crystal structure on the surface with 1.6 kcal/mol relaxation energy; in the second step, one of the surface $NH_4^+N_3O_4^-$ molecules undergoes proton transfer and desorbs as the molecular complex $H_3N\cdots HON(O)NNO_2$ with a 29.4 kcal/mol barrier without an intrinsic transition state; in the last step, the molecular complex $H_3N\cdots HON(O)$-NNO_2 dissociates rapidly to NH_3 and $HON(O)NNO_2$ with 13.9 kcal/mol endothermicity also without a distinct barrier. The rate constant for the last two steps have been calculated. The predicted overall sublimation activation energy and the rate constant are in reasonable agreement with most of the available experimental data. Furthermore the effect of water on ADN sublimation is quite different from that on AP; the sublimation enthalpies for $(H_2O)_x$--NH_4/N_3O_4 (x = 0, 1, 2, 3), 29.4, 32.6, 32.8, and 30.0 kcal/mol, are larger than the values 28.1, 21.4, 18.6, and 14.2 kcal/mol for $(H_2O)_x$−NH_4/ClO_4 (x = 0, 1, 2, 3).

■ ASSOCIATED CONTENT

Ⓢ Supporting Information

Structures of the $NH_4^+[ON(O)NNO_2]^-$ and $[NH_4]^+[N(NNO_2)]^-$; structural parameters for the sublimation products without and with 2 H_2O molecules on the AP and ADN surfaces; key vibrational frequencies for the NH_4/N_3O_4 pair in the relaxed surface and in the transition state involved in the sublimation process; vibrational frequencies for the gas-phase species calculated at the B3LYP/6-311+G(3df,2p) level; variational dissociation curve of $[H_3N]-[HON(O)NNO_2]$ (g) → NH_3 (g) + $HON(O)NNO_2$ (g). This material is available free of charge via the Internet at http://pubs.acs.org.

AUTHOR INFORMATION

Corresponding Author

*E-mail: chemmcl@emory.edu.

Notes

The authors declare no competing financial interest.

ACKNOWLEDGMENTS

This work was supported by the Office of Naval Research under grant No. N00014-08-1-0106. M.C.L. gratefully acknowledges the supports from Taiwan's MOE ATU program as well as the National Science Council and the Taiwan Semiconductor Manufacturing Co. for the NSC-distinguished visiting professorship and the TSMC distinguished professorship respectively at the Center for Interdisciplinary Molecular Science, National Chiao Tung University, Hsinchu, Taiwan. We are very much indebted to Taiwan's National Center for High-performance Computing for the extensive CPU's needed in this work.

REFERENCES

(1) Giles, J. *Nature* **2004**, *427*, 580−581.
(2) Bottaro, J. C.; Penwell, P. E.; Schmitt, R. J. *J. Am. Chem. Soc.* **1997**, *19*, 9405−9410.
(3) Christe, K. O.; Wilson, W. W.; Petrie, M. A.; Michels, H. H.; Bottaro, J. C.; Gilardi, R. *Inorg. Chem.* **1996**, *25*, 5068−5071.
(4) Russell, T. P.; Piermari, G. J.; Block, S.; Miller, P. J. *J. Phys. Chem.* **1996**, *100*, 3248−3251.
(5) Gilardi, R.; Flippen-Anderson, J.; George, C.; Butcher, R. J. *J. Am. Chem. Soc.* **1997**, *119*, 9411−9416 and references herein..
(6) Pavlov, A. N.; Grebennikov, V. N.; Nazina, L. D.; Nazin, G. M.; Manelis, G. B. *Russ. Chem. Bull.* **1999**, *48*, 50−54.
(7) Vyazovkin, S.; Wight, C. A. *J. Phyc. Chem. A* **1997**, *101*, 5653−5658.
(8) Tompa, A. S. *Thermochim. Acta* **2000**, *375*, 177−193.
(9) Oxley, J. C.; Smith, J. L.; Zheng, W.; Rogers, E.; Coburn, M. D. *J. Phys. Chem. A* **1997**, *101*, 5646−5652.
(10) Korobeinichev, O. P.; Kuibida, L. V.; Paletsky, A. A.; Shmakov, A. G. *J. Propulsion Power* **1998**, *14*, 991−1000.
(11) Politzer, P.; Seminario, J.; Concha, M. *J. Mol. Struct.: Theochem.* **1998**, *427*, 123−129.
(12) Mebel, A. M.; Lin, M. C.; Morokuma, K.; Melius, C. F. *J. Phys. Chem.* **1995**, *99*, 6842−6848.
(13) Park, J.; Chakraborty, D.; Lin, M. C. *27th Symp. (Int.) on Combustion* **1998**, 2351−2357.
(14) Zhu, R. S.; Wang, J. H.; Lin, M. C. *J. Phys. Chem. C* **2007**, *111*, 13831−1383.
(15) Zhu, R. S.; Lin, M. C. *J. Phys. Chem. C* **2008**, *112*, 14481−14485.
(16) Kresse, G.; Hafner, J. *Phys. Rev. B* **1993**, *47*, 558−561.
(17) Kresse, G.; Hafner, J. *Phys. Rev. B* **1994**, *49*, 1425−14269.
(18) Kresse, G.; Furthmuller, J. *Comput. Mater. Sci.* **1996**, *6*, 15−50.
(19) Kresse, G.; Furthmuller, J. *Phys. Rev. B* **1996**, *54*, 11169−11186.
(20) Perdew, J. P.; Yang, Y. *Phys. Rev. B.* **1992**, *45*, 244−13249.
(21) Lee, C.; Yang, W.; Parr, R. G. *Phys. Rev. B.* **1988**, *37*, 785−789.
(22) Monkhorst, H.; Pack, J. *Phys. Rev. B.* **1976**, *13*, 5188−5192.
(23) Laidler, K. J. *Theories of Chemical Reaction Rates*; McGraw-Hill: London, 1969, Ch. 3.
(24) Hsu, C. −C.; Mebel, A. M.; Lin, M. C. *J. Chem. Phys.* **1996**, *105*, 2346−2352.
(25) Chakraborty, D.; Hsu, C.-C.; Lin, M. C. *J. Chem. Phys.* **1998**, *109*, 8889−8898.
(26) Mokrushin, V.; Bedanov, Tsang, W.; Zachariah, M. R.; Knyazev, V. D. *ChemRate, Version 1.19*; National Institute of Standards and Technology: Gaithersburg, MD 20899, 2002.
(27) Gilbert, R. G.; Smith, S. C. *Theory of Unimolecular and Recombination Reactions*; Blackwell Scientific: Carlton, Australia, 1990.
(28) Holbrook, K. A.; Pilling, K. J.; Robertson, S. H. *Unimolecular Reactions*; Wiley: Chichester, U.K., 1996.
(29) Wardlaw, D. M.; Marcus, R. A. *Chem. Phys. Lett.* **1984**, *110*, 230−234.
(30) Klippenstein, S. J.; Wagner, A. F.; Dunbar, R. C.; Wardlaw, D. M. Robertson, S. H. *VARIFLEX: VERSION 1.00*, 1999.
(31) Zhu, R. S.; Lin, M. C. *Int. J. Energetic Materials & Chem. Prop.* **2010**, *9*, 493−504.
(32) Kazakov, A. I.; Rubtsov, Y. I.; Manelis, G. B. *Propel., Expl., Pyrotech.* **1999**, *24*, 37−42.
(33) Kazakov, A. I.; Rubtsov, Y. I.; Andrienko, L. P.; Manelis, G. B. *Russ. Chem. Bull.* **1998**, *47*, 379−385.
(34) Ochterski, J. W.; Petersson, G. A.; Montgomery, J. A., Jr. *J. Chem. Phys.* **1996**, *104*, 2598−619.
(35) Montgomery, J. A., Jr.; Frisch, M. J.; Ochterski, J. W.; Petersson, G. A. *J. Chem. Phys.* **2000**, *112*, 6532−42.